

Long-Lived, Directional Photoinduced Charge Separation in Ru^{II} Complexes Bearing Laminate Polypyridyl Ligands

Marek B. Majewski,^[a] Norma R. de Tacconi,^[b] Frederick M. MacDonnell,^{*[b]} and Michael O. Wolf^{*[a]}

Abstract: Ru^{II} complexes incorporating both amide-linked bithiophene donor ancillary ligands and laminate acceptor ligands; dipyrido[3,2-a:2',3'-c]phenazine (dppz), tetrapyrido[3,2-a:2',3'-c:3'',2''-h:2''',3'''-j]phenazine (tpphz), and 9,11,20,22-tetraazatetrapyrido[3,2-a:2',3'-c:3'',2''-l:2''',3''']-pentacene (tatpp) exhibit long-lived charge separated (CS) states, which have been analyzed using time-resolved transient absorption (TA), fluorescence, and electronic absorption spectroscopy in addition to ground state electrochemical and spectroelectrochemical measurements. These complexes possess two electronically relevant ³MLCT states related to electron occupation of MOs localized predominantly on the proximal “bpy-like” portion and central (or

distal) “phenazine-like” portion of the acceptor ligand as well as energetically similar ³LC and ³ILCT states. The unusually long excited state lifetimes (τ up to 7 μ s) observed in these complexes reflect an equilibration of the ³MLCT_{prox} or ³MLCT_{dist} states with additional triplet states, including a ³LC state and a ³ILCT state that formally localizes a hole on the bithiophene moiety and an electron on the laminate acceptor ligand. Coordination of a Zn^{II} ion to the open coordination site of the laminate acceptor ligand is observed to

significantly lower the energy of the ³MLCT_{dist} state by decreasing the magnitude of the excited state dipole and resulting in much shorter excited state lifetimes. The presence of the bithiophene donor group is reported to substantially extend the lifetime of these Zn adducts via formation of a ³ILCT state that can equilibrate with the ³MLCT_{dist} state. In tpphz complexes, Zn^{II} coordination can reorder the energy of the ³MLCT_{prox} and ³MLCT_{dist} states such that there is a distinct switch from one state to the other. The net result is a series of complexes that are capable of forming CS states with electron–hole spatial separation of up to 14 Å and possess exceptionally long lifetimes by equilibration with other triplet states.

Keywords: charge transfer • donor–acceptor systems • energy conversion • photochemistry • photophysics

Introduction

The guiding principles behind the design of effective artificial systems for photochemical energy conversion are built on foundations established by electron transfer (ET) research and investigations into natural photosynthetic processes. In Photosystem II, photoexcitation initiates a cascade of ET reactions spatially separating the electron–hole pair such that this energy can be used to drive multi-electron water oxidation and carbon fixation reactions.^[1] Attempts to mimic photosynthesis have led to the study of molecular

donor–chromophore (D–C) or chromophore–acceptor (C–A) dyads, donor–chromophore–acceptor (D–C–A) triads, and more elaborate tetrads, pentads, and related multimodular assemblies.^[2] These assemblies are designed to support directional long-range electron transfer upon photoexcitation with the goal of producing high energy redox equivalents for follow-on reactions. Such efforts are still hampered by fast recombination rates and competing relaxation processes, such as energy transfer, radiative and nonradiative decay.^[3] In general, charge separated (CS) states in molecular triads are relatively short lived, with lifetimes ranging from tens to hundreds of nanoseconds.^[4] In linear, rod-like D–C–A molecular triads capable of directional charge separation, modest increases in charge separated state lifetimes (up to ~1 μ s) have been achieved by maximizing the separation distance of the electron–hole pair and have been further enhanced by applying some external perturbation (hydrogen bonding, for example).^[5]

One strategy to increase the lifetime of the charge separated state is by equilibration with other low-lying states.^[6] There are numerous reports of extending the lifetime of the triplet metal-to-ligand charge transfer state (³MLCT) in Ru^{II} polypyridyl complexes by excited state equilibration with ligand centered triplet states (³LC).^[7] Previously, we have re-

[a] M. B. Majewski, Prof. M. O. Wolf
Department of Chemistry, University of British Columbia
2036 Main Mall, Vancouver, BC, V6T 1Z1 (Canada)
Fax: (+1) 604-822-2847
E-mail: mwolf@chem.ubc.ca

[b] Dr. N. R. de Tacconi, Prof. F. M. MacDonnell
Department of Chemistry and Biochemistry
University of Texas at Arlington, 700 Planetarium Place
Arlington, TX, 76019-0065 (USA)
Fax: (+1) 817-272-3808
E-mail: macdonn@uta.edu

Supporting information for this article is available on the WWW under <http://dx.doi.org/10.1002/chem.201203786>.

ported that incorporation of bithienyl groups into Ru^{II} polypyridyl complexes results in a long-lived charge separated state fueled by a ³LC state.^[8] Although high in energy ($\Delta G \approx 2.0$ eV) these systems lack the characteristic vectorial charge transfer observed in Photosystem II, and electron-hole pairs formed on photoexcitation are localized in relatively close spatial proximity.

In this study, we have paired the bithienyl functionality with Ru^{II} polypyridyl complexes containing “laminar” acceptor ligands (Figure 1): dipyrido[3,2-a:2',3'-c]phenazine

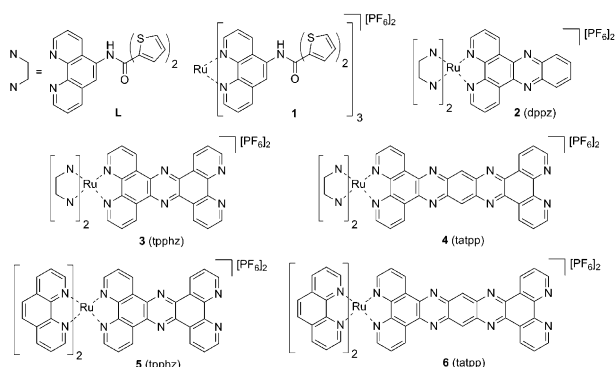


Figure 1. Complexes discussed in this work.

(dppz), tetrapyrrodo[3,2-a:2',3'-c:3'',2''-h:2''',3''''-j]phenazine (tpphz), and 9,11,20,22-tetraazatetrapyrrodo[3,2-a:2',3'-c:3'',2''-l:2''',3''''-p]pentacene (tatpp). Laminar acceptor ligands have two or more acceptor orbitals that are delocalized over the entire ligand (laminated over each other) but interact with the metal such that one orbital defines the ground state optical properties of the complex (referred to as the “optical” molecular orbital) and the other orbital defines the ground state reduction potentials (referred to as the “redox” molecular orbital).^[9,10] For example, the lowest energy ¹MLCT transition (~ 2.7 eV) in $[(\text{phen})_2\text{Ru}(\text{dppz})]^{2+}$ (phen = 1,10-phenanthroline) is assigned to a Ru $d\pi \rightarrow \pi^*$ (dppz LUMO + 1) transition, whereas the reduction process for the $[(\text{phen})_2\text{Ru}(\text{dppz})]^{2+/+}$ couple occurs at -0.83 V versus Ag/AgCl (Table 1) and is assigned to populating the LUMO localized on dppz.^[11] In this case the LUMO + 1 corresponds to the optical orbital where the majority of the orbital density is localized on the bipyridine-like portion responsible for metal chelation and for this reason it is often also referred to as the proximal molecular orbital. The LUMO (or redox molecular orbital) is one where the majority of the orbital density is localized on the

“phenazine-like” or distal portion of the dppz ligand (also referred to as the distal MO). In the excited state, these two acceptor MOs (both proximal and distal) participate to give ³MLCT_{prox} and ³MLCT_{dist} states, either of which may dominate the excited state properties of the complex depending on solvent, secondary coordination sphere, protonation, or in the case of tatpp and tpphz ligands, metalation at the open end.^[12] Thus, in the MLCT excited state, the laminar ligands offer two potential sites of electron storage with the distal site formally storing an electron spatially further away from the Ru^{III} center.

Complexes bearing dppz and tpphz ligands are well studied largely due to the “light-switch effect”, referring to the observation that bright emission from the ³MLCT_{prox} state is observed in aprotic solvents or when the complex is intercalated into DNA.^[12b,13] In protic solvents, these complexes are only weakly emissive due to the low quantum yield of emission associated with the ³MLCT_{dist} state (the dominant state in protic environments).^[10b,14] The mechanism of this switching effect is still contested; however, it is clearly dependent on the solvent dipole and H-donor capacity.^[10b,11,12c,14,15] From the temperature dependence of the luminescence in CH₃CN, Brenneman and co-workers have shown that the excited state equilibrium between the ³MLCT_{prox} and ³MLCT_{dist} states in $[(\text{phen})_2\text{Ru}(\text{dppz})]^{2+}$ is shifted to the proximal state due to entropic effects, illustrating how energetically close the two states are in this medium.^[12a] In some cases, the lifetimes of these ³MLCT states are also enhanced through excited-state equilibration with ligand-centered (³LC) states on the laminar ligands. For example, the lifetime of the ³MLCT_{dist} state in $[(\text{phen})_2\text{Ru}(\text{tatpp})\text{Ru}(\text{phen})_2]^{4+}$ is extended to 1.3 μs in CH₂Cl₂ by equilibration with a ³LC state on the tatpp ligand.^[12f] Although the lowest energy excited state is largely ³LC in nature, the complex retains much of the reactivity and excited state properties of the ³MLCT state.

In this work, we have prepared D–C–A triads (Figure 1) by incorporating amide-linked bithienyl donor ancillary ligands (L) and a series of linear acceptor ligands into Ru^{II} complexes **2–4**. Here, bithienyl moieties may act as reduc-

Table 1. Redox potentials for the oxidation (E_{ox}) and reduction (E_{red}) of the complexes.

Compound	E_{ox} (Ru ^{2+/3+})	E_{ox} (BT ^{0/+})	E_{red} redox MO	E_{red} redox MO	E_{red} optical MO
$[\text{Ru}(\text{phen})_3]^{2+}$ ^[19]	1.35		-1.37		-1.37
1 ^[8]	1.35	1.25	-1.50		-1.50
2 (dppz)			-0.98 ^[a]		-1.19
$[(\text{phen})_2\text{Ru}(\text{dppz})]^{2+}$	1.38		-0.83	-1.28	-1.46
3 (tpphz)	1.37	1.24	-0.77	-1.06	-1.53
4 (tatpp)	1.37	1.25	-0.28/-0.33 ^[a, b]	-0.47/-0.44 ^[a, b]	-1.19
5 (tpphz) ^[20]	1.38		-0.82		-1.28
6 (tatpp) ^[21]	1.33		-0.30	-0.83	-1.38
$[(\text{phen})_2\text{Ru}(\text{tpphz})\text{Ru}(\text{phen})_2]^{4+}$ ^[20]	1.38		-0.67		-1.27
$[(\text{phen})_2\text{Ru}(\text{tatpp})\text{Ru}(\text{phen})_2]^{4+}$ ^[21] (7)	1.39		-0.22	-0.71	-1.28
Zn(tatpp)Zn ⁴⁺ adduct ^[22]			0.04	-0.25	

All potentials are quoted versus Ag/AgCl reference electrode in CH₃CN except potentials for **3**, which are quoted versus Ag/AgNO₃. [a] Data estimated from SEC data. [b] Splitting of the first redox process due to π - π stacking.^[21]

tive quenchers for Ru^{III} formed on photoexcitation and the excited electron may be directed to either the proximal or distal MO on the acceptor ligand. In this respect, it is possible to represent these species as tetrads D–C–A–A'. If the electron is directed to the distal MO, the resulting interligand charge transfer (ILCT) state would nominally represent a charge-separated state with 11 to 14 Å (center of the acceptor ligand to the center of the bithienyl moiety) separating the electron–hole pair, a distance at which back electron transfer (BET) may be slowed.^[16] In some cases, incorporation of bithienyl groups may introduce additional low-lying ³LC states that can extend the lifetime of low-lying CS states through excited state equilibration (the “triplet reservoir” effect),^[7c] making the CS state available to follow-on reactions. Here, we report on the excited-state processes observed in these triads and our success in the preparation of assemblies exhibiting long-lived excited states and directional charge separation, making them useful models for the study of biomimetic photoinduced electron transfer.

Results and Discussion

Synthesis and characterization: Mononuclear complexes **2** and **3** were prepared according to literature procedures reported for their unsubstituted 2,2'-bipyridine (bpy)/1,10-phenanthroline (phen) analogues.^[17] Complex **4** was prepared by condensation of [Ru(L)₂(1,10-phenanthroline-5,6-dione)]-[PF₆]₂ with dipyrido[3,2-a:2',3'-c]phenazine-11,12-diamine in CH₃CN/glacial AcOH/EtOH. All complexes were isolated as hexafluorophosphate salts and structures were confirmed by NMR spectroscopy and high resolution mass spectrometry. At moderate concentrations, complexes **3** and **4** show broad ¹H NMR signals associated with aggregation via π–π stacking of the polypyridyl tphz and tatpp moieties.^[18] To resolve the ¹H NMR spectra, five equivalents of Zn^{II} as Zn(OTf)₂ was added to prepared NMR samples which has the effect of coordinating the open end of the complex and breaking up the π–π stacking as evidenced by a sharpening of the NMR peaks (Figure S1 in the Supporting Information).

Electrochemical evaluation: Electrochemical data for complexes **1–6** and important related complexes are collected in Table 1 and schematically represented in Figure 2. The data in Table 1 were predominantly obtained by either CV or DPV techniques, however, in some instances the reductive processes in the dppz- and tatpp-based complexes are not clearly observed by these techniques and are only detected as minor quasi-irreversible waves, particularly tatpp complexes in the presence of Zn^{II}. We presume that this difficulty is associated with poor surface electron-transfer kinetics and/or absorption effects. It is clear that a redox process is occurring in many such cases, as we observe clear optical changes in the absorption spectra using transmittance spectroelectrochemical (SEC) techniques. It is then practical to estimate the potential of a poorly defined redox process in

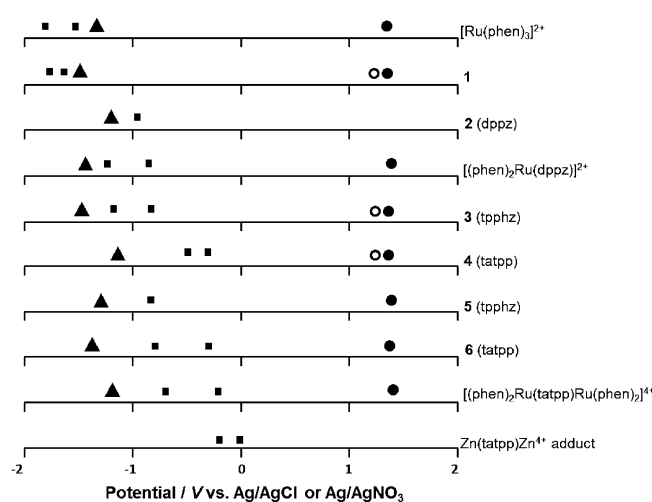


Figure 2. Schematic comparison of the redox potentials of the reported complexes; Ru^{2+/3+} oxidation (●), bithienyl oxidation (○), ligand-based reductions associated with the distal (redox) MO (■) and proximal (optical) MO (▲).

CV or DPV by SEC, which tracks the spectral changes of solution species. These data are included in Table 1 and are specifically noted.

It is well-established that the energies of MLCT absorption in most Ru^{II} polypyridyl complexes correlate linearly with the difference between the electrochemical potentials for (metal-centered) oxidation and (ligand-centered) reduction.^[23] In these cases, the redox MO and the optical MO are the same. In complexes with laminate acceptor ligands, it is generally the second or third reduction potential that reveals the energy of the optical MO and these values are perturbed to more negative potentials than anticipated due to Coulombic effects. Nevertheless, the difference in the Ru^{2+/3+} potential and the reduction potential of the proximal (or optical) MO does correspond well with the optical data (¹MLCT_{prox} typically centered at ~460 nm). The observation of the redox MO reduction prior to reduction of the optical MO is a clear measure that the redox MO is the ground state LUMO. Complexes with bithienyl (BT) moieties also exhibit an irreversible oxidative process associated with the BT^{0/+} couple at approximately +1.25 V, assigned to formation of the bithienyl radical cation and subsequent polymerization reactions.^[8] This process is observed prior to and overlapping with the Ru^{2+/3+} couple (typically observed at ~1.35 V) indicating that the HOMO in bithienyl adducts is the bithiophene MO, not the Ru dπ MOs. It is apparent from the optical data (see below) that the Ru dπ MO acts as the donor orbital in the observed lowest energy optical transitions (i.e., the ¹MLCT bands centered at 460 nm).

Ground state optical properties: The ground state absorption spectra of complexes **2–4** (Figure 3) exhibit features analogous to those of their unsubstituted analogues, [(phen)₂Ru(dppz)]²⁺,^[11] **5**, and **6** (Figure S2 in the Supporting Information). Absorption spectra of **2–4** exhibit moder-

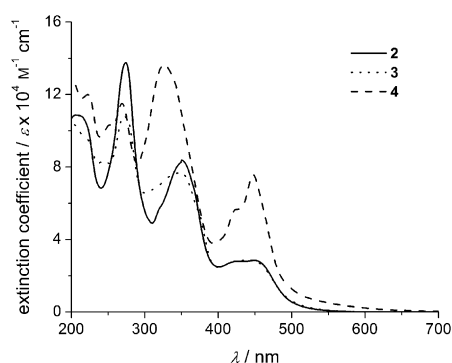


Figure 3. Absorbance spectra of complexes 2–4 in CH₃CN.

ately intense Ru $d\pi \rightarrow \pi^*$ $^1\text{MLCT}$ transitions in the visible region (centered around 460 nm). Because the energy of these transitions are essentially identical to the corresponding $^1\text{MLCT}$ transitions in $[\text{Ru}(\text{phen})_3]^{2+}$, they can be assigned to the $^1\text{MLCT}_{\text{prox}}$ state in which the electron resides in a “bpy-like” proximal MO. MLCT transitions between the Ru^{II} $d\pi(\text{HOMO}) \rightarrow \pi^*$ redox or distal MO are expected to be of considerably lower energy on the basis of electrochemical measurements and are not observed in any of the complexes. The UV region of these spectra is dominated by LC transitions, with a strong bithiophene $\pi \rightarrow \pi^*$ transition centered at 355 nm. In complexes 3 and 4, this bithiophene transition overlaps with LC transitions localized on tpphz and tatpp moieties. Additionally tatpp complexes (4, 6, and 7) all exhibit an intense structured band at 445 nm overlapping with the $^1\text{MLCT}_{\text{prox}}$ transition.^[12f] Coordination of Zn^{II} to the open chelation site in 3–6, causes only minor perturbations in the visible region of the ground state absorption spectra (Figure S3 in the Supporting Information). It becomes clear, however, that this coordination has a significant effect on the excited state relaxation processes.

Excited state properties: Excitation of these complexes at wavelengths corresponding to their lowest-lying transitions, typically the $^1\text{MLCT}$ transitions, results in emission centered at approximately 610 nm in 2, 3, and 5, whereas complexes 4 and 6 exhibit no detectable emission. The energy of the emission in 2 and 3 matches that observed for related complexes without bithienyl groups, $[(\text{phen})_2\text{Ru}(\text{dppz})]^{2+}$ and 5, that has previously been assigned to emission from a $^3\text{MLCT}_{\text{prox}}$ state.^[11,20] Addition of Zn^{II} to 3 and 5 reduces the

intensity of emission and shifts the emission maximum to 660 nm (Figure S4 in the Supporting Information); this is indicative of switching emission from the $^3\text{MLCT}_{\text{prox}}$ to the $^3\text{MLCT}_{\text{dist}}$ state. This metalation-induced switching effect was previously reported for the bpy analogue of 5, $[(\text{bpy})_2\text{Ru}(\text{tpphz})]^{2+}$ when bound to DNA.^[15d] The ruthenium dimer, $[(\text{phen})_2\text{Ru}(\text{tpphz})\text{Ru}(\text{phen})_2]^{4+}$ (7), represents the extreme case which is permanently metalated at both ends and consequently, emission from 7 at 710–740 nm has been interpreted as emission from the $^3\text{MLCT}_{\text{dist}}$ state.^[15d,25] Complexes 4 and 6 remain non-emissive when Zn^{II} is added, which is consistent with this $^3\text{MLCT}_{\text{dist}}$ state always lying significantly lower in energy than the $^3\text{MLCT}_{\text{prox}}$ in complexes incorporating tatpp. The lack of emission is due to the low energy nature of this state, which may be expected to emit in the near IR region or decay rapidly and nonradiatively.

Determining the exact nature of the excited state in these complexes requires analysis of luminescence lifetimes (τ_{em}) along with quantum yields (Φ_{em}) and excited state lifetimes (τ_{es}) measured by time resolved transient absorption (TA) spectroscopy (Table 2). Where data exist for both τ_{em} and τ_{es} the values are generally in good agreement. Importantly, τ_{es} data offer insight into excited state processes even when the compound is nonemissive.

Table 2. Summary of photophysical properties of complexes.

Compound	λ_{em} [nm]	Φ_{em}	τ_{em} [μs] ^[a]	τ_{es} [μs] ^[b]
$\text{Ru}(\text{phen})_3^{2+}$	600	0.036 ^[d]	0.523	0.528
1 ^[8]	600	0.072	7.4	6.2
2 (dppz)	615	0.110	2.2	2.2
$[(\text{phen})_2\text{Ru}(\text{dppz})]^{2+}$	600 ^[11]	0.033 ^[11]	0.66 ^[11]	
3 (tpphz)	614	0.044 ^[d]	3.6 (0.27)	4.5 (388–488 nm) 3.5 (520–650 nm) 0.095 (433–483 nm) 0.131 (570–620 nm)
3Zn (tpphz-Zn ²⁺)	661			0.095 (433–483 nm) 0.131 (570–620 nm) 5.8–7.0 ^[c]
4 (tatpp)				0.10–0.15 ^[c]
4Zn (tatpp-Zn ²⁺)				0.891
5 (tpphz)	604	0.073 ^[20]	0.900	0.081 (433–483 nm) 0.090 (570–620 nm)
5Zn (tpphz-Zn ²⁺)	658			0.35–0.55 ^[c] 0.004
6 (tatpp)				0.005 (CH ₃ CN) 1.30 (CH ₂ Cl ₂) ^[12f]
6Zn (tatpp-Zn ²⁺)				30 ^[12f]
$[(\text{phen})_2\text{Ru}(\text{tatpp})\text{Ru}(\text{phen})_2]^{4+}$ (7)				
“Zn(tatpp)Zn ⁴⁺ adduct				

All measurements were recorded in CH₃CN unless otherwise noted, solutions prepared in air and then purged with Ar for 15 min: [a] $\lambda_{\text{ex}} = 453$ nm; [b] $\lambda_{\text{ex}} = 355$ nm. [c] Different regions of the spectrum have differing lifetimes. [d] Calculated by comparison to $[\text{Ru}(\text{bpy})_3]^{2+}$.^[24]

Over the series of complexes, there is a tremendous variation in excited state lifetimes as measured by emission and TA methods. Significantly, we observe that complexes with appended bithienyl groups exhibit considerably longer lifetimes than their unsubstituted analogues. Previously, complex 1 was compared to $[\text{Ru}(\text{phen})_3]^{2+}$, and the observed lifetime extension was attributed to excited state equilibration of a bithienyl ligand triple state ($^3\text{LC}_{\text{BT}}$) and an intraligand charge transfer state ($^3\text{ILCT}$) with the $^3\text{MLCT}$ state.^[8]

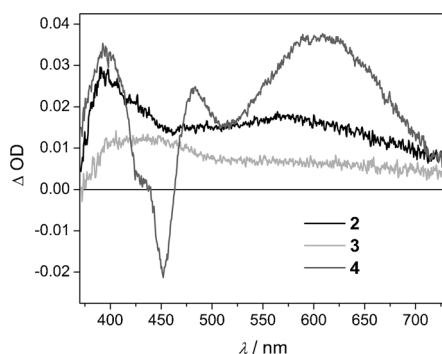


Figure 4. TA difference spectra of **2–4** in CH₃CN ($t=0.78\text{--}1.28\ \mu\text{s}$, fwhm = 35 ps).

In the remaining complexes in this study, we observe the bi-thienyl moieties playing a similar role, albeit not always involving both the $^3\text{LC}_{\text{BT}}$ and $^3\text{ILCT}$ states. This is illustrated in Figure 4, in which the TA difference spectra of complexes **2**, **3**, and **4** at t approximately 1 μs are overlaid. For **2** and **3**, the most notable feature in these spectra is the absence of a MLCT bleach in the 430–480 nm region, indicating that the predominant excited state is not a MLCT-based state but rather a $^3\text{LC}_{\text{BT}}$ state in equilibrium with a $^3\text{MLCT}_{\text{prox}}$ state, (as evidenced by emission at $\sim 610\ \text{nm}$). Comparing emission energies, it is reasonable to suggest that in **2** and **3** the $^3\text{MLCT}_{\text{prox}}$ state is nearly isoenergetic with the $^3\text{LC}_{\text{BT}}$ and $^3\text{ILCT}$ states observed in **1**, suggesting the BT is playing a similar role in **2** and **3**; behaving both as a triplet reservoir, and a reductive quencher for Ru^{III}.

Solvent and Zn^{II} coordination effects in unsubstituted tatpp complexes: The TA difference spectrum observed for **4** (Figure 4), is essentially identical to that reported for the tatpp ^3LC state in [(phen)₂Ru(tatpp)Ru(phen)₂]⁴⁺ (**7**).^[12f] However, the excited state lifetime of **4** (in CH₃CN) is much longer than that reported for **7** (6 vs. 0.005 μs). To fully understand the nature of the excited state manifold in triad complexes **2–4** and Zn^{II} adducts of **3** and **4**, it is necessary to first understand the excited state processes in their unsubstituted analogues, [(phen)₂Ru(dppz)]²⁺, **5**, **6**, and **7**.

The sensitivity of excited state decay processes to solvent is most clearly seen in the “light-switch” behavior reported for [(bpy)₂Ru(dppz)]²⁺ and [(phen)₂Ru(dppz)]²⁺ wherein addition of protic solvents to CH₃CN solutions of these complexes switches emission from a “bright” $^3\text{MLCT}_{\text{prox}}$ state to a “dark” $^3\text{MLCT}_{\text{dist}}$ state, which is weakly emissive. Conversely, the dark state can be switched to the bright state in an aqueous solution by addition of DNA. In both cases, the ability of solvent to access and stabilize the excited state dipoles generated is understood to be involved in the light switch behavior. Because protic solvents can interact with the excited state through protonation or H bonding in addition to simple dipolar stabilization, their role is not fully understood.^[11,26] The behavior of complex **7** exemplifies how sensitive the MLCT states can be to changes in solvent dipole in the absence of proton donors. Dinuclear complex

7 has a Ru^{II} ion coordinated to both chelation sites of the tatpp ligand and from electrochemical data it is clear that the energy of the redox orbital is appreciably lower (by approximately 1 eV) than the optical MO. In this case, it is clear that the $^3\text{MLCT}_{\text{dist}}$ state is always lower in energy than the $^3\text{MLCT}_{\text{prox}}$ state and that the $^3\text{MLCT}_{\text{prox}}$ state is not noticeably involved in the relaxation process other than as a conduit to the $^3\text{MLCT}_{\text{dist}}$ state or other lower-lying states. One such lower-lying state is a ^3LC state centered on tatpp which is also observed in TA spectra for the Zn(tatpp)Zn⁴⁺ adduct. The tatpp ligand is insoluble in most common organic solvents but readily dissolves in CH₃CN on addition of Zn^{II}. The non-luminescent $^3\text{LC}_{\text{tatpp}}$ excited state has a lifetime of $\tau_{\text{es}} \approx 30\ \mu\text{s}$ and the TA spectrum reported for the Zn^{II} adduct is essentially identical to that of **7*** in CH₂Cl₂ at 1 μs .^[12f] From this and the lifetime data, the Jablonski diagram in Figure 5 was proposed by Chiorboli et al.^[12f] Excitation of **7** into absorption bands corresponding to either the $^1\text{MLCT}$ state or the ^1LC states of the tatpp ligand quickly leads to population of a $^3\text{LC}_{\text{tatpp}}$ state.^[12f] In CH₂Cl₂, the lifetime of this state is 1.3 μs but upon switching to CH₃CN, this lifetime drops to <1 ns. This change in lifetime is due to equilibration between the energetically similar $^3\text{LC}_{\text{tatpp}}$ and $^3\text{MLCT}_{\text{dist}}$ states, which will exhibit an overall lifetime that is a weighted average of the population of the two individual states (ca. 30 μs for $^3\text{LC}_{\text{tatpp}}$ and ca. 250 ps for $^3\text{MLCT}_{\text{dist}}$).^[11] Because a large dipole is induced in the $^3\text{MLCT}_{\text{dist}}$ state, this state is more stable in polar solvents than in nonpolar solvents that influence the ΔE between the two equilibrating states as indicated in Figure 5 (left panel). The shortened lifetime of **7*** in more polar solvents reflects a decrease in the ΔE from 0.21 eV in CH₂Cl₂ to 0.03 eV in CH₃CN, as calculated using a two-state model.^[27]

Complex **6** exhibits a similar kind of switching behavior, except that metalation at the open end may be used to stabilize the energy of the $^3\text{MLCT}_{\text{dist}}$ state relative to the $^3\text{LC}_{\text{tatpp}}$ state. The TA spectrum of **6** reveals that the $^3\text{LC}_{\text{tatpp}}$ state is also the predominantly occupied state in **6*** (Figure S5 in the Supporting Information).^[12f] The Jablonski diagram for **6** (Figure 5, right panel), shows qualitatively similar behavior to **7** but for different reasons. In this case, the absence of a second Ru^{II} center raises the energy of the $^3\text{MLCT}_{\text{dist}}$ state to lie 0.18 eV above the $^3\text{LC}_{\text{tatpp}}$ state in CH₃CN, as determined from the lifetimes. Addition of Zn^{II} shortens the lifetime, from 400 to 4 ns, corresponding to a decrease in ΔE from 0.18 to 0.06 eV. This is almost the same ΔE as seen for the ruthenium dimer **7** in CH₃CN showing that coordination of the Zn^{II} ion in place of the Ru^{II} ion, yields nearly identical results.

Zn^{II} coordination and BT substituent effects in tpphz complexes: The TA spectra of complexes **3** and **5** in CH₃CN are overlaid in Figure 6a, and those of the corresponding Zn^{II} adducts, **3Zn** and **5Zn**, are shown in Figure 6b. The striking difference between the TA difference spectra of **3** and **5** reveals the significant variation in the nature of their excited states. In **5**, the strong ground state MLCT bleach centered

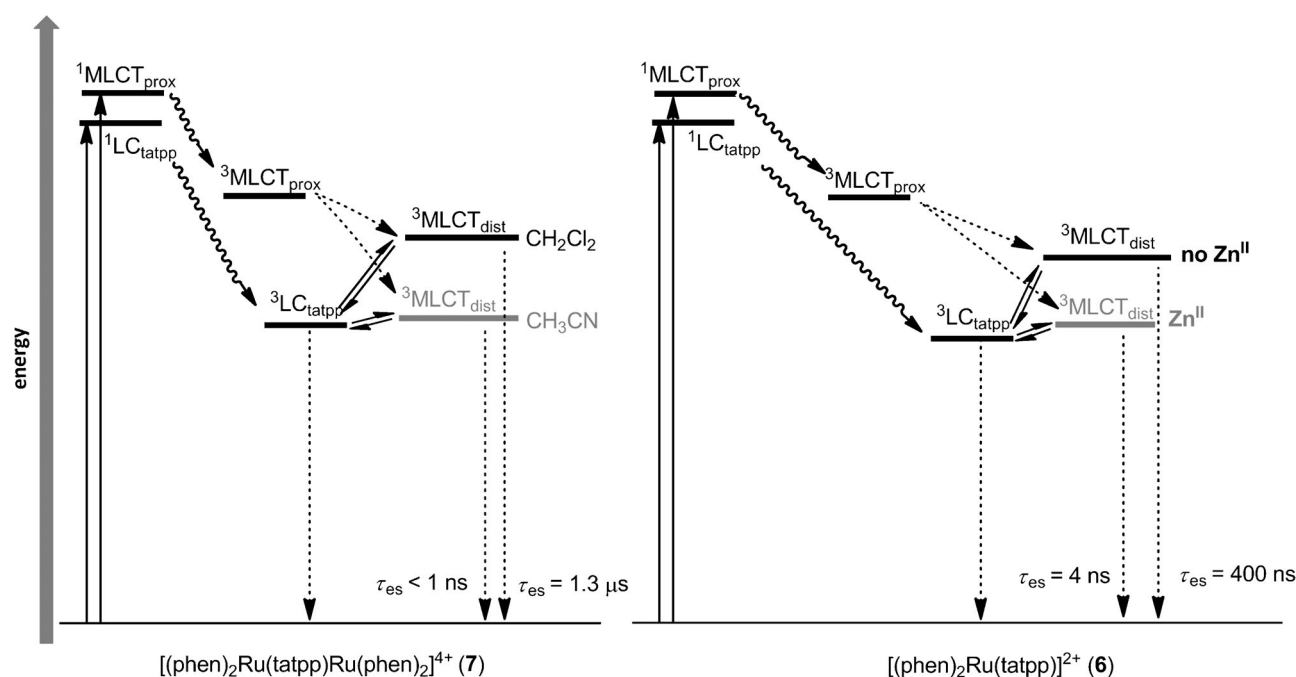


Figure 5. Qualitative Jablonski diagrams of **7** (left) in CH_3CN or CH_2Cl_2 and **6** (right) in CH_3CN . On the left, the gray highlights are used to show how the $^3\text{MLCT}_{\text{dist}}$ is perturbed by the solvent, CH_2Cl_2 (black) or CH_3CN (gray). On the right, the gray highlights are used to show how the $^3\text{MLCT}_{\text{dist}}$ is perturbed by the presence (gray) or absence (black) of Zn^{II} . Dashed arrows are used to indicate non-radiative decay pathways.

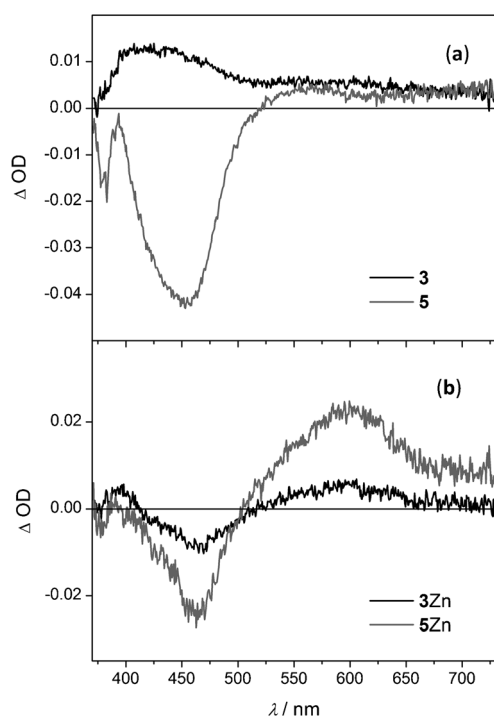


Figure 6. a) TA difference spectra of **3** and **5** ($t=551\text{--}1048$ ns); b) TA difference spectra of **3** and **5** in the presence of 5 equiv Zn^{II} ($t=61\text{--}111$ ns).

between 400–500 nm indicates that the final excited state resembles a $^3\text{MLCT}$ state (where the Ru^{II} center has been converted to Ru^{III}).^[28] A relatively high energy emission at 604 nm and a moderately long lifetime of 900 ns allows the

assignment of the excited state in **5** as a $^3\text{MLCT}_{\text{prox}}$ excited state.^[15e,29] In **3**, the MLCT bleach is not observed, indicating that the predominant excited state species is not a MLCT state (with Ru^{III}), however, the observed emission at 614 nm and extended lifetime of 3.6 μs indicate that the predominant excited state is long-lived and is being depleted by an excited-state equilibration process with the $^3\text{MLCT}_{\text{prox}}$ state. Figure 7 shows Jablonski diagrams indicating the relevant excited states and their interactions for the Zn^{II} -adduct and Zn^{II} -free complexes, **5Zn** and **5** (Figure 7, left panel) and **3Zn** and **3** (Figure 7, right panel). In **5**, the $^3\text{MLCT}_{\text{prox}}$ state is the predominant excited state on the nanosecond time-scale. On the other hand, the adduct **5Zn** exhibits luminescence at 660 nm and a shortened lifetime ($\tau_{\text{es}}=90$ ns) that are indicative of formation of a $^3\text{MLCT}_{\text{dist}}$ state, which has been stabilized by Zn^{II} coordination.

The dominant excited state observed in **3** is a $^3\text{LC}_{\text{BT}}$ state which is characterized, in part, by absorption in the TA difference spectrum at 420–440 nm (Figure 6a) and a lifetime enhancement. The observed emission at 614 nm indicates this $^3\text{LC}_{\text{BT}}$ state decays through thermal population of a $^3\text{MLCT}_{\text{prox}}$ state (Figure 7, right panel). In the case of **3**, the $^3\text{MLCT}_{\text{dist}}$ state is higher in energy than the $^3\text{MLCT}_{\text{prox}}$ state and plays no significant role in the excited-state processes. As with complex **5**, coordination of Zn^{II} to **3** lowers the energy of the $^3\text{MLCT}_{\text{dist}}$ state to below that of the $^3\text{MLCT}_{\text{prox}}$ state as evidenced by emission at 661 nm. Significantly, the lifetime of adduct **3Zn** ($\tau_{\text{es}}=950$ ns) is considerably longer than that of **5Zn** ($\tau_{\text{es}}=90$ ns), and the TA spectra (Figure 6b) exhibit similar features, albeit less intense in **3Zn**. We propose that the lifetime enhancement could be due to

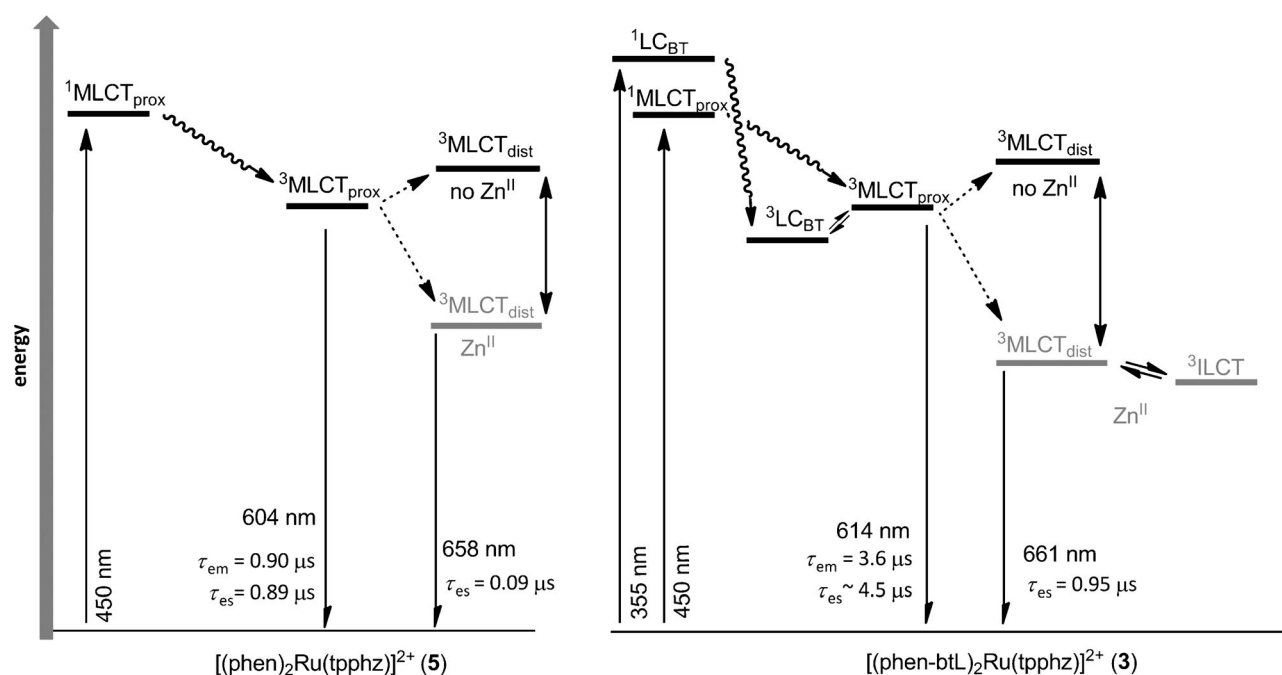


Figure 7. Qualitative Jablonski diagrams of **5** (left) in CH₃CN and **3** (right) in CH₃CN. In both diagrams, the gray highlights are used to show how the ³MLCT_{dist} is perturbed through the addition (gray) or lack (black) of Zn^{II}.

excited-state equilibration of the ³MLCT_{dist} with a ³ILCT state in which the hole is formally localized on a BT moiety and an electron is localized in the distal tpphz MO. A clearly observable positive feature is seen at 400 nm in the **3**Zn spectrum that is absent in **5**Zn and may be attributed to a BT radical cation.^[30] Rapid electron transfer between the neutral BT and an adjacent Ru^{III} ion in the ³MLCT_{dist} state would be needed for generation of the aforementioned ³ILCT state. A comparison of ground state redox potentials for Ru^{2+/3+} and BT^{0/+} reveals that the two couples are less than 0.1 V apart and that oxidation of the BT moiety by the Ru^{III} is exergonic. Reduction of the distal tpphz orbital, as would be found in the excited state complex **3**Zn*, should not alter this situation appreciably. We can rule out the potential role of a low-lying ³LC_{tpphz} state being responsible for the enhanced lifetimes as this should affect both **3**Zn and **5**Zn equally, and the energy of this state is likely too high to be involved as the free ligand, tpphz, emits at 380 nm (3.15 eV) in CH₂Cl₂.^[31]

The light switching behavior of [(bpy)₂Ru(tpphz)]²⁺ (a 2,2'-bipyridine analogue of **5**) in CH₃CN when either protonated with strong acids or metalated (with Ru^{II} and Os^{II}) was first reported by Chiroboli et al.^[15d,32] Similar switching behavior is seen when [(bpy)₂Ru(tpphz)]²⁺ is bound to DNA in the presence or absence of Zn^{II} or Co^{II}.^[15d] In this latter case, it seems that the DNA-bound state essentially approximates the solvent environment of CH₃CN. The behavior of **7**, **6**, **6**Zn, **5** and **5**Zn, as a function of solvent and metalation with Zn^{II} (of which only **5** and **5**Zn show actual light-switch behavior) reveals that the principal way in which Zn^{II} modifies the excited state properties is by modulation of the magnitude of excited state dipole moments, es-

pecially with respect to the ³MLCT_{dist} state. The relative magnitude of the excited state dipoles (μ) in [(phen)₂Ru³⁺(tpphz⁻)]^{2+*} (**5***) would be $\mu(^3\text{MLCT}_{\text{dist}}) > \mu(^3\text{MLCT}_{\text{prox}})$. Equilibration between the ³MLCT_{prox} and ³MLCT_{dist} states is shifted to favor the former in less polar solvents and the latter in solvents of greater polarity. Upon formation of the **5**Zn adduct the linear Ru(+3)–tpphz(–1)–Zn(+2) charge configuration in the excited state results in opposed internal dipoles which partially cancel out, resulting in a much smaller excited dipole compared to the Ru(+3)–tpphz(–1) dipole in **5***. In this excited state, the magnitudes of the dipoles are always considerably smaller and the energy of the ³MLCT_{dist} is always lower than that of the ³MLCT_{prox}, regardless of the solvent polarity. In other words, in **5**Zn the charge separated state (³MLCT_{dist}) is the preferred state as the presence of the Zn^{II} at the opposite end of the tpphz ligand results in a Coulombic well that “pulls” the electron towards an orbital in the center of the tpphz ligand.

As discussed below, this is slightly different to the outcome of Zn^{II} (or Ru^{II}) coordination in tatpp complexes **6**Zn and **7** where metalation at the open site serves to modulate ΔE between a ³LC_{tatpp} state and the ³MLCT_{dist} state. The net effect is to stabilize the ³MLCT_{dist} state, which would now be the lowest energy state relative to the ³LC state in **7***, resulting in shortening of the excited state lifetime as the equilibrium is shifted to favor the state with the shortest lifetime.

Zn^{II} coordination and BT substituent effects in tatpp complexes: The TA spectra of complexes Zn(tatpp)Zn⁴⁺, **4**, and **4**Zn in CH₃CN are overlaid in Figure 8a, and Figure 8b shows the TA spectrum of **4** overlaid with **6** (along with the

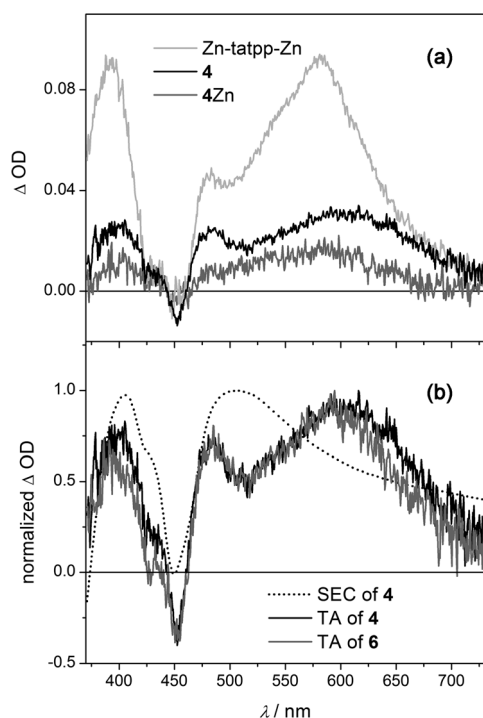


Figure 8. a) TA spectra of the Zn(tatpp)Zn⁴⁺ adduct ($t \sim 1 \mu\text{s}$), **4** ($t = 456\text{--}647 \text{ ns}$) and **4Zn** ($t = 61\text{--}111 \text{ ns}$) in CH₃CN; b) reductive SEC of **4** (-0.9 V) and TA difference spectra of **4** ($t = 456\text{--}647 \text{ ns}$) and **6** ($t = 43\text{--}243 \text{ ns}$) in CH₃CN.

reductive SEC of **4**). It is immediately clear that all of the TA spectra resemble the spectrum of the Zn(tatpp)Zn⁴⁺ adduct, and that this spectrum must correspond to the ³LC_{tatpp} state reported by Chiroboli et al.^[12f] This spectrum features a bleach of the LC transition at 445 nm and three positive features: one feature at higher energy (380–420 nm) and two features at lower energies (480 nm and a broad feature between 550–650 nm). Electrochemical reduction (Figure 8b) of the tatpp ligand in **4** to form [L₂Ru^{II}(tatpp⁻)]⁺ was observed to bleach the LC transition at 445 nm and give two positive peaks at approximately 400 and 520 nm, which correspond to a ³MLCT_{dis} state but also correlate well with two of the three features observed in the ³LC_{tatpp} state. It appears that the broad low energy peak at 620 nm is a unique characteristic of the LC triplet state. None of the tatpp complexes are observed to luminesce under any conditions, due to quantitative population of the low-lying ³LC_{tatpp} state regardless of the solvent or metalation state of the complex.

In CH₃CN, all of the Ru^{II}-tatpp complexes have lifetimes on the 1–400 ns timescale, with the notable exception of BT complex **4** ($\tau_{\text{es}} \approx 6 \mu\text{s}$). A comparison of these data with the TA data for **6**, the previous data for **1–3**, **7**, and the associated Zn adducts, illustrates that we have designed and built a triad capable of both vectorial charge transfer and long-lived CS state. Figure 9 shows the qualitative Jablonski diagrams for **4** and **4Zn** derived from our understanding of these data. This diagram is very similar to that shown for **6** (Figure 5, right panel) except for the new states introduced by addition of the BT moieties. Regardless of the excitation

channel, the system undergoes intersystem crossing and relaxation to yield a ³LC_{tatpp} state, as seen from TA data in the sub-500 ns regime (Figure 8b). The lifetime of this state changes from 6 μs without Zn^{II} to 100 ns with Zn^{II}, a 60-fold decrease. As seen in **6**^{*}, this strong dependence on the presence or absence of Zn^{II} is understood within the framework of the ³MLCT_{dis} state accelerating the decay process by depleting the ³LC_{tatpp} state through excited state equilibration. The energies of the ³MLCT_{dis} states in Zn^{II}-free **4** (black) and **4Zn** (grey) relative to the ³LC_{tatpp} state are shown in Figure 9.

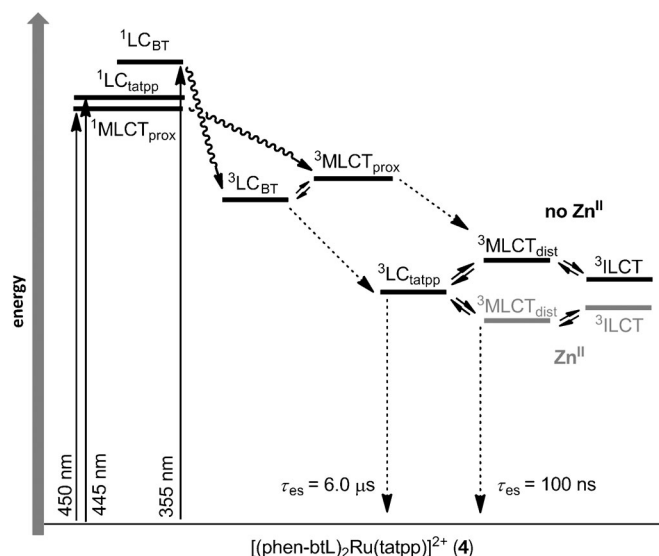


Figure 9. Qualitative Jablonski diagrams of **4** and **4Zn** in CH₃CN. The grey highlights are used to show which states are most perturbed by the presence or absence of Zn^{II}. A grey highlight shows the relative energy level of a state in the presence of Zn^{II}. Dashed arrows are used to indicate non-radiative decay pathways.

Given that the appended BT moieties are spatially far away from the tatpp ligand, we would expect the energies of these states to be similar to those found in **6**, (Figure 5, right panel). In **4**, however, the presence of BT groups extends the lifetime in **4**^{*} to 6 μs compared to 450 ns in **6**^{*}. It is very unlikely that the ³MLCT_{prox} or ³LC_{BT} states are involved in lifetime enhancement as they are too high in energy to equilibrate with the ³LC_{tatpp} or ³MLCT_{dis} states. We suggest that the change from phen in **6** to **L** in **4** is either raising the energy of the ³MLCT_{dis} or introducing a new low energy ³ILCT state which is now equilibrating with the ³MLCT_{dis} and ³LC_{tatpp} states (Figure 9).

In this new ³ILCT state the hole on Ru^{III} in the ³MLCT_{dis} state hops to the BT moiety to form the BT radical cation and the excited state electron is localized in the distal tatpp MO. Another possibility is one resulting from an increase in the energy of the ³MLCT_{dis} state in **4** (and **4Zn**) relative to the same state in **6** (and **6Zn**). It is possible that the change from phen to **L** alters the Ru^{2+/3+} oxidation potential such that the energy of the ³MLCT_{dis} state increases relative to

the ³LC_{tatpp} state and thereby increases the observed excited state lifetime. Using a two-state model, we can calculate that an increase of 0.072 eV in the energy gap of **4*** relative to **6*** would account for the observed increase in lifetime. This is not an unreasonable increase given that the ground state oxidation potentials for the Ru^{2+/3+} couple are observed to vary by as much as 50 mV for the compounds in Table 1. However, when the oxidation potentials of the homoleptic complexes [Ru(phen)₃]²⁺ and [RuL₃]²⁺ (**1**) are compared, no change is observed. Similarly, when the Ru^{2+/3+} oxidation potentials of **4** and **6** are compared, only a 40 mV difference is observed, not the 72 mV needed to account for the longer lifetime. Although these data suggest that the perturbation to the energy of the ³MLCT_{dist} in **4*** is not enough to account for the observed increase in excited state lifetime, the error associated with measuring these oxidation potentials is significant enough that it is hard to make conclusions based on these data alone.

An additional argument can be made that the increase in Ru^{2+/3+} oxidation potential in **4Zn** should be the same as seen in **4**. It has been previously shown for both [(phen)₂Ru(tpphz)Ru(phen)₂]⁴⁺ and **7** that the Ru^{2+/3+} couples are independent and observed as a single two-electron wave, meaning that the presence of a second metal ion at this remote site does not alter the Ru^{2+/3+} oxidation potential due to Coulombic effects (it does, however, alter the energy of the tpphz or tatpp reduction potential as expected). Thus, Zn^{II} coordination at the distal site in **4Zn** or **6Zn** should not alter the Ru^{2+/3+} potential. If this is the case, then the Ru^{2+/3+} oxidation potential in **4** and **4Zn** should be identical and, as such, the increase in the ΔE (³MLCT_{dist} to ³LC_{tatpp}) in **4Zn** relative to **6Zn** is calculated to give an enhanced lifetime of 69 ns (using the two state model), whereas the observed lifetime is 100 ns. In this respect, the data are not consistent with a two-state model. The introduction of a ³ILCT state to give a three equilibrating excited state model is unusual but not unprecedented.^[33] It is clear from ground state redox data that formation of the ³ILCT state is exergonic from the ³MLCT_{dist} state by as much as 0.1 eV and mechanistically it is easy to rationalize a simple electron transfer from the BT moiety to the Ru^{III} site. We note that a similar extension of excited state lifetime was seen in tpphz complexes **3** and **3Zn** relative to **5** and **5Zn** due to the presence of BT moieties. As with the tatpp complexes, this extension could be due to either a change in the Ru^{2+/3+} oxidation potential or the presence of a ³ILCT state (Figure 9). Although it is not possible to definitively assign the source of the increase in the excited state lifetime of **4**, **4Zn**, and **3Zn** to the presence of a ³ILCT state, the data support this interpretation.

Conclusion

The design of triads for light-induced charge separation must address two important factors: the degree or distance of charge separation, and the amount of energy stored in

the final CS state. In complex **3**, the ³MLCT_{prox} state has approximately the same energy (2.0 eV) as the ³MLCT state in [Ru(phen)₃]²⁺, however, in both cases the actual distance of charge separation is small, as the MLCT state involved has a minimal distance of charge separation (~3 Å, centroid of the phen to the Ru^{III} site). In **3Zn**, there is a nominal increase in the distance of charge separation to 6.2 Å for the ³MLCT_{dist} state (centroid of the tpphz ligand to the Ru^{III} site). The energy of this state can be estimated from the emission data at 1.67 eV.^[34] This correlates well with the energy of this state estimated from the difference in potential between the Ru^{2+/3+} couple at +1.38 V and the first ligand reduction in [(phen)₂Ru(tpphz)Ru(phen)₂]⁴⁺ at -0.73 V^[35] which gives 1.51 eV. The energy of the ³ILCT state would be approximately 0.1 eV lower at 1.41 eV but further increases the distance of charge separation to approximately 11 Å (centroid of the extended BT moiety to the centroid of the tpphz ligand).

The excited states in the tatpp complexes are nonluminescent so the energies of the excited states must be estimated using the ground state redox potentials (as was done for **3Zn**). In this case we obtain an excited state energy of approximately 1.08 eV for the ³MLCT_{dist} state and about 0.98 eV for the ³ILCT state in **4**. These values drop by approximately 0.08 eV for the Zn^{II} adduct **4Zn** but still indicate an appreciable amount of stored energy. Although there is a loss of 0.5 eV on going from the tpphz to tatpp complexes, the distance of charge separation has increased to about 14 Å (centroid of the BT moiety to the centroid of the tatpp ligand). If the electron can be transferred via binding of a substrate to the open tatpp site in **4** or by coordination of the substrate to the Zn^{II} in **4Zn**, the effective charge separation distance of this transient species would measure over 20 Å. Given the long-lived and directional charge separated nature of the excited state in complexes bearing tatpp and tpphz acceptor ligands, these structures may be used as the site of primary charge separation in artificial photosynthetic assemblies.

Experimental Section

General: All solvents and reagents including those for NMR analysis (Cambridge Isotope Laboratories) were obtained from commercial sources and used as received except where noted. NMR spectra were recorded on either a Bruker AV400-Direct, Bruker AV400-Indirect (400 MHz) or Bruker AV600 (600 MHz) spectrometer. All chemical shifts are referenced to residual solvent signals, which were previously referenced to tetramethylsilane. Splitting patterns are designated as s (singlet), d (doublet), t (triplet), m (multiplet). ESI-MS (Bruker Esquire) and MALDI-TOF MS (Bruker Biflex IV) were acquired at the UBC Microanalysis facility. UV/Vis absorption spectra were obtained with a Varian Cary 5000 using Fisher (HPLC Grade) solvents. Fluorescence data were collected on a Photon Technology International (PTI) fluorimeter using a 75 W Xe arc lamp as the source. Absolute quantum yields were determined using an integrating sphere coupled to the PTI fluorimeter. Fluorescence lifetime measurements were carried out using a Horiba Jobin Yvon TBX picosecond photon detection module (Nanoled λ_{ex} = 453 nm). Transient absorbance spectra were collected using a Princeton Instruments Spectra Pro 2300i Imaging Triple Grating Monochromator/Spectrograph with a

Hamamatsu Dynamic Range Streak Camera (excitation source: EKSPLA PL2241 Nd:YAG laser, $\lambda_{\text{ex}}=355$ nm, fwhm=35 ps). Where wavelengths other than 355 nm were required, an EKSPLA Model PG401 picosecond optical parametric generator was pumped at 355 nm by a PL2241 mode-locked laser to produce wavelengths from 420–680 nm (Signal) and 720–2300 nm (Idler). Electrochemical data were obtained on a CHI620C electrochemical analyzer (CH Instruments, Austin, TX, USA). A single-compartment, three-electrode electrochemical cell was used with either a glassy carbon (1.5 mm diameter disk) or platinum (1.0 mm diameter disk) from Cypress Systems as working electrode. Immediately before use, the electrode was polished to a mirror finish with wet alumina (Buehler, 0.05 μm), followed by rinsing with Millipore Milli-Q water and sonication. A Pt wire and a nonleak Ag/AgCl, satd. KCl reference electrode (Cypress Systems, model EE009) were used as counter and reference electrodes, respectively. All potentials were measured and are quoted versus Ag|AgCl|satd. KCl reference electrode. All electrochemical data were recorded in acetonitrile with 0.1 M Bu₄NPF₆ as supporting electrolyte. Cyclic voltammetry (CV) and differential pulse voltammetry (DPV) were used for the electrochemical characterization of respective complexes. Transmittance spectroelectrochemical measurements were performed at constant potential in a quartz thin-layer compartment containing a platinum minigrad as working electrode. The liquid thin layer was spectroscopically probed as a function of time by using a diode array spectrometer (Hewlett–Packard model 8453). The counter electrode (platinum wire) and the Ag/AgCl reference electrode were placed in the quartz cuvette near to the thin layer compartment.

Synthesis: The preparation of ligand **L** has been previously reported.^[8] Complexes **2** and **3** were prepared according to modified published literature procedure.^[17] Ru(L)₂Cl₂^[36] [Ru(L)₂(1,10-phenanthroline-5,6-dione)]-[PF₆]₂^[37] dipyrido[3,2-a:2',3'-c]phenazine-11,12-diamine (dadppz) (Scheme S1 in the Supporting Information) used in the preparation of **4** were also prepared using modified literature procedures. Complexes **5** and **6** were prepared as described in the literature.^[17b,38]

[Ru(L)₂(dppz)][PF₆]₂ (2): Complex **2** was purified by silica gel column chromatography with CH₃CN/H₂O/KNO_{3(aq)} (96:3:1) as eluent. Yield: 0.051 g (27%). ¹H NMR (400 MHz, [D₃]acetonitrile): $\delta=7.13$ (dt, $J=5.18, 3.50$ Hz, 1H), 7.36–7.41 (m, 1H), 7.44 (t, $J=3.35$ Hz, 1H), 7.48 (dt, $J=3.27, 1.87$ Hz, 1H), 7.61–7.74 (m, 2H), 7.77–7.87 (m, 1H), 7.91–7.95 (m, 1H), 8.02–8.06 (m, 1H), 8.11–8.20 (m, 3H), 8.24–8.28 (m, 1H), 8.49 (dd, $J=6.40, 3.35$ Hz, 1H), 8.52 (s, 1H), 8.61 (d, $J=8.22$ Hz, 1H), 8.74 (ddd, $J=8.53, 3.65, 0.91$ Hz, 1H), 9.31 (d, $J=2.13$ Hz, 1H), 9.67 ppm (dd, $J=8.22, 1.22$ Hz, 1H); ¹³C NMR (150.92 MHz, [D₃]acetonitrile): $\delta=121.59, 121.65, 124.05, 124.89, 125.30, 125.74, 126.47, 126.84, 127.34, 128.11, 129.19, 130.71, 130.36, 132.08, 133.09, 133.22, 135.38, 136.17, 139.59, 142.31, 142.97, 145.81, 147.8, 150.40, 152.07, 152.30, 152.96, 153.12, 153.81, 160.66$ ppm. HR-ESI MS (m/z): [M]⁺ calcd for C₆₀H₃₆N₁₀O₂F₆PS₄Ru: 1300.0610; found: 1300.0607 (0.2 ppm).

[Ru(L)₂(tpphz)][PF₆]₂ (3): Complex **3** was obtained as an orange solid, washed with (2 mL) H₂O, EtOH and Et₂O and used without further purification. Yield: 17 mg (77%). ¹H NMR (3+5 equiv Zn^{II}, 400 MHz, [D₃]acetonitrile): $\delta=7.11$ (m, 1H), 7.39 (m, 3H), 7.68 (m, 2H), 7.82 (m, 1H), 7.94 (m, 3H), 8.29 (m, 1H), 8.39 (dd, $J=8.22, 4.87$ Hz, 1H), 8.50 (m, 1H), 8.60 (d, 1H), 8.75 (m, 1H), 9.37 (d, $J=4.87$ Hz, 1H), 9.47 (br s, 1H), 9.96 (d, $J=7.31$ Hz, 1H), 10.23 ppm (d, $J=8.53$ Hz, 1H); ¹³C NMR (3+5 equiv Zn²⁺, 100.63 MHz, [D₃]acetonitrile): $\delta=123.72, 125.88, 126.90, 127.09, 127.57, 128.25, 128.70, 129.71, 129.91, 131.40, 132.04, 132.24, 135.01, 135.47, 137.22, 138.03, 141.56, 141.78, 143.67, 144.75, 148.44, 149.29, 149.63, 151.61, 152.07, 154.99, 156.38, 158.92, 159.12, 161.62$ ppm. HR-ESI MS (m/z): [M]⁺ calcd for C₆₆H₃₈N₁₂O₂F₆PS₄Ru: 1402.0818; found: 1402.0825 (−0.5 ppm).

[Ru(L)₂(tatpp)][PF₆]₂ (4): [Ru(L)₂(1,10-phenanthroline-5,6-dione)][PF₆]₂ (20.0 mg, 1.45×10^{-5} mol) was dissolved in CH₃CN (15 mL) and added dropwise to a solution of dadppz (5.5 mg, 1.7×10^{-5} mol, Scheme S1 in the Supporting Information) in glacial acetic acid/EtOH (1:1, 60 mL) heated to reflux. The suspension was left heated to reflux for 12 h and then filtered hot. The filtrate was concentrated to approximately 15 mL and an aqueous solution of NH₄PF₆ was added resulting in precipitation of a dark brown solid. The solid was isolated by filtration and washed

with small volumes (2 mL) or H₂O, EtOH and Et₂O. This product was used without further purification. Yield: 19 mg (79%). ¹H NMR (4+5 equiv Zn^{II}, 400 MHz, [D₃]acetonitrile): $\delta=7.14$ (m, 1H), 7.40 (m, 1H), 7.45 (t, $J=4.42$ Hz, 1H), 7.49 (t, $J=4.72$ Hz, 1H), 7.70 (m, 2H), 7.87 (ddd, $J=8.15, 5.25, 3.35$ Hz, 1H), 7.95 (t, 4.26, 1H), 8.05 (m, 1H), 8.13 (m, 1H), 8.19 (t, 1H), 8.27 (m, 1H), 8.35 (d, $J=5.48$ Hz, 1H), 8.53 (d, $J=9.75$ Hz, 1H), 8.64 (dd, $J=8.38, 3.50$ Hz, 1H), 8.77 (d, $J=8.83$ Hz, 1H), 8.99 (d, $J=4.26$ Hz, 1H), 9.37 (d, $J=2.74$ Hz, 1H), 9.73 (m, 2H), 10.05 ppm (d, $J=7.92$ Hz, 1H). HR-ESI MS (m/z): [M–H]⁺ calcd for C₇₂H₃₉N₁₄O₂S₄Ru: 1358.1294; found: 1358.1323 (−2.1 ppm).

Acknowledgements

The authors acknowledge the NSERC (M.O.W.), NSF (CHE0911720, F.M.M.), Robert A. Welch Foundation (Y-1301, F.M.M.), and Mountain Equipment Co-op (M.B.M.) for support. We thank Dr. Saeid Kamal (UBC-LASIR) for assistance with TA measurements.

- [1] J. Barber, *Chem. Soc. Rev.* **2009**, *38*, 185–196.
- [2] a) J. D. Megiato, Jr., A. Antoniuk-Pablant, B. D. Sherman, G. Kodis, M. Gervald, T. A. Moore, A. L. Moore, D. Gust, *Proc. Natl. Acad. Sci. USA* **2012**, *109*, 15578–15583; b) L. L. Tinker, N. D. McDaniel, S. Bernhard, *J. Mater. Chem.* **2009**, *19*, 3328–3337; c) J. P. Sauvage, J. P. Collin, J. C. Chambron, S. Guillerez, C. Coudret, V. Balzani, F. Barigelletti, L. De Cola, L. Flamigni, *Chem. Rev.* **1994**, *94*, 993–1019; d) S. Campagna, G. Denti, S. Serroni, A. Juris, M. Venturi, V. Ricevuto, V. Balzani, *Chem. Eur. J.* **1995**, *1*, 211–221; e) M. E. El-Khouly, C. A. Wijesinghe, V. N. Nesterov, M. E. Zandler, S. Fukuzumi, F. D'Souza, *Chem. Eur. J.* **2012**, *18*, 13844–13853.
- [3] a) D. Gust, T. A. Moore, A. L. Moore, *Acc. Chem. Res.* **2009**, *42*, 1890–1898; b) A. C. Benniston, A. Harriman, *Materials Today* **2008**, *11*, 26–34.
- [4] a) G. Kodis, P. A. Liddell, L. de La Garza, A. L. Moore, T. A. Moore, D. Gust, *J. Mater. Chem.* **2002**, *12*, 2100–2108; b) R. Berera, G. F. Moore, I. H. van Stokkum, G. Kodis, P. A. Liddell, M. Gervald, R. van Grondelle, J. T. M. Kennis, D. Gust, T. A. Moore, A. L. Moore, *Photochem. Photobiol. Sci.* **2006**, *5*, 1142–1149; c) A. C. Benniston, A. Harriman, P. Li, P. V. Patel, C. A. Sams, *Chem. Eur. J.* **2008**, *14*, 1710–1717; d) M. Ogawa, B. Balan, G. Ajayakumar, S. Maskaoka, H.-B. Kraatz, M. Muramatsu, S. Ito, Y. Nagasawa, H. Miyasaka, K. Sakai, *Dalton Trans.* **2010**, *39*, 4421–4434.
- [5] a) J. Hankache, M. Niemi, H. Lemmetyinen, O. S. Wenger, *Inorg. Chem.* **2012**, *51*, 6333–6344; b) J. Hankache, M. Niemi, H. Lemmetyinen, O. S. Wenger, *J. Phys. Chem. A* **2012**, *116*, 8159–8168.
- [6] X.-y. Wang, A. Del Guerto, R. H. Schmehl, *J. Photochem. Photobiol. C* **2004**, *5*, 55–77.
- [7] a) J. Gu, J. Chen, R. H. Schmehl, *J. Am. Chem. Soc.* **2010**, *132*, 7338–7346; b) S. Ji, W. Wu, W. Wu, P. Song, K. Han, Z. Wang, S. Liu, H. Guo, J. Zhao, *J. Mater. Chem.* **2010**, *20*, 1953–1963; c) A. F. Morales, G. Accorsi, N. Armaroli, F. Barigelletti, S. J. A. Pope, M. D. Ward, *Inorg. Chem.* **2002**, *41*, 6711–6719; d) D. S. Tyson, K. B. Henbest, J. Bialecki, F. N. Castellano, *J. Phys. Chem. A* **2001**, *105*, 8154–8161.
- [8] M. B. Majewski, N. R. de Tacconi, F. M. MacDonnell, M. O. Wolf, *Inorg. Chem.* **2011**, *50*, 9939–9941.
- [9] S. Singh, N. R. de Tacconi, N. R. G. Diaz, R. O. Lezna, J. Muñoz Zuñiga, K. Abayan, F. M. MacDonnell, *Inorg. Chem.* **2011**, *50*, 9318–9328.
- [10] a) J. Fees, M. Ketterle, A. Klein, J. Fiedler, W. Kaim, *J. Chem. Soc. Dalton Trans.* **1999**, 2595–2600; b) J. Fees, W. Kaim, M. Moscherosch, W. Matheis, J. Klima, M. Krejciak, S. Zalis, *Inorg. Chem.* **1993**, *32*, 166–174.
- [11] E. J. C. Olson, D. Hu, A. Hörmann, A. M. Jonkman, M. R. Arkin, E. D. A. Stemp, J. K. Barton, P. F. Barbara, *J. Am. Chem. Soc.* **1997**, *119*, 11458–11467.

- [12] a) M. K. Brennaman, J. H. Alstrum-Acevedo, C. N. Fleming, P. Jang, T. J. Meyer, J. M. Papanikolas, *J. Am. Chem. Soc.* **2002**, *124*, 15094–15098; b) A. E. Friedman, J. C. Chambron, J. P. Sauvage, N. J. Turro, J. K. Barton, *J. Am. Chem. Soc.* **1990**, *112*, 4960–4962; c) Y. Sun, C. Turro, *Inorg. Chem.* **2010**, *49*, 5025–5032; d) M. Bräutigam, M. Wächtler, S. Rau, J. Popp, B. Dietzek, *J. Phys. Chem. C* **2011**, *115*, 1274–1281; e) C. Chiorboli, M. A. J. Rodgers, F. Scandola, *J. Am. Chem. Soc.* **2003**, *125*, 483–491; f) C. Chiorboli, S. Fracasso, M. Ravaglia, F. Scandola, S. Campagna, K. L. Wouters, R. Konduri, F. M. MacDonnell, *Inorg. Chem.* **2005**, *44*, 8368–8378.
- [13] C. Hiort, P. Lincoln, B. Norden, *J. Am. Chem. Soc.* **1993**, *115*, 3448–3454.
- [14] M. K. Brennaman, T. J. Meyer, J. M. Papanikolas, *J. Phys. Chem. A* **2004**, *108*, 9938–9944.
- [15] a) C. G. Coates, J. Olofsson, M. Coletti, J. J. McGarvey, B. Önfelt, P. Lincoln, B. Norden, E. Tuite, P. Matousek, A. W. Parker, *J. Phys. Chem. B* **2001**, *105*, 12653–12664; b) B. Önfelt, J. Olofsson, P. Lincoln, B. Nordén, *J. Phys. Chem. A* **2003**, *107*, 1000–1009; c) J. Olofsson, B. Önfelt, P. Lincoln, *J. Phys. Chem. A* **2004**, *108*, 4391–4398; d) Y. Liu, A. Chouai, N. N. Degtyareva, D. A. Lutterman, K. R. Dunbar, C. Turro, *J. Am. Chem. Soc.* **2005**, *127*, 10796–10797; e) M. Schwalbe, M. Karnahl, S. Tschierlei, U. Uhlemann, M. Schmitt, B. Dietzek, J. Popp, R. Groake, J. G. Vos, S. Rau, *Dalton Trans.* **2010**, *39*, 2768–2771.
- [16] O. S. Wenger, *Acc. Chem. Res.* **2011**, *44*, 25–35.
- [17] a) E. Amouyal, A. Homsí, J.-C. Chambron, J.-P. Sauvage, *J. Chem. Soc. Dalton Trans.* **1990**, 1841–1845; b) J. Bolger, A. Gourdon, E. Ishow, J.-P. Launay, *Inorg. Chem.* **1996**, *35*, 2937–2944.
- [18] X. Xie, S. P. Mulcahy, E. Meggers, *Inorg. Chem.* **2009**, *48*, 1053–1061.
- [19] F. Barigelletti, A. Juris, V. Balzani, P. Belser, A. Von Zelewsky, *Inorg. Chem.* **1987**, *26*, 4115–4119.
- [20] S. Campagna, S. Serroni, S. Bodige, F. M. MacDonnell, *Inorg. Chem.* **1999**, *38*, 692–701.
- [21] N. R. de Tacconi, R. Chitakunye, F. M. MacDonnell, R. O. Lezna, *J. Phys. Chem. A* **2008**, *112*, 497–507.
- [22] R. O. Lezna, N. R. de Tacconi, T. Janaratne, J. Muñoz Zúñiga, F. M. MacDonnell, *J. Argent. Chem. Soc.* **2009**, *97*, 273–288.
- [23] A. Juris, V. Balzani, F. Barigelletti, S. Campagna, P. Belser, A. von Zelewsky, *Coord. Chem. Rev.* **1988**, *84*, 85–277.
- [24] J. M. Calvert, J. V. Caspar, R. A. Binstead, T. D. Westmoreland, T. J. Meyer, *J. Am. Chem. Soc.* **1982**, *104*, 6620–6627.
- [25] L. Flamigni, S. Encinas, F. Barigelletti, F. M. MacDonnell, K.-J. Kim, F. Puntoriero, S. Campagna, *Chem. Commun.* **2000**, 1185–1186.
- [26] C. Turro, S. H. Bossmann, Y. Jenkins, J. K. Barton, N. J. Turro, *J. Am. Chem. Soc.* **1995**, *117*, 9026–9032.
- [27] J. E. Yarnell, J. C. Deaton, C. E. McCusker, F. N. Castellano, *Inorg. Chem.* **2011**, *50*, 7820–7830.
- [28] C. Turró, Y. C. Chung, N. Leventis, M. E. Kuchenmeister, P. J. Wagner, G. E. Leroi, *Inorg. Chem.* **1996**, *35*, 5104–5106.
- [29] R. B. Nair, B. M. Cullum, C. J. Murphy, *Inorg. Chem.* **1997**, *36*, 962–965.
- [30] a) Y. Yagci, S. Jockusch, N. J. Turro, *Macromolecules* **2007**, *40*, 4481–4485; b) T. Keszthelyi, M. M. L. Grage, J. F. Offersgaard, R. Wilbrandt, C. Svendsen, O. S. Mortensen, J. K. Pedersen, H. J. A. Jensen, *J. Phys. Chem. A* **2000**, *104*, 2808–2823.
- [31] M. Karnahl, S. Tschierlei, C. Kuhnt, B. Dietzek, M. Schmitt, J. Popp, M. Schwalbe, S. Kriech, H. Gork, F. W. Heinemann, S. Rau, *Dalton Trans.* **2010**, *39*, 2359–2370.
- [32] C. Chiorboli, C. A. Bignozzi, F. Scandola, E. Ishow, A. Gourdon, J.-P. Launay, *Inorg. Chem.* **1999**, *38*, 2402–2410.
- [33] Y. Leydet, D. M. Bassani, G. Jonusauskas, N. D. McClenaghan, *J. Am. Chem. Soc.* **2007**, *129*, 8688–8689.
- [34] Although the emission maximum of 661 nm suggests an even higher energy should be possible, previously reported data for the dinuclear ruthenium complex [(phen)₂Ru(tpphz)Ru(phen)₂]⁴⁺ in CH₃CN yields an emission maximum closer to 740 nm giving an energy of the ³MLCT_{dist} state at 1.67 eV, when two metals are bound. Higher energy maxima are seen when “mixing” occurs with mononuclear complex [(phen)₂Ru(tpphz)]²⁺; see ref. [15d].
- [35] Assigned to reduction of the distal or redox MO, at –0.73 V and correcting for intersystem crossing (–0.6 eV taken from the loss observed during intersystem crossing in [Ru(phen)₃]²⁺).
- [36] B. P. Sullivan, D. J. Salmon, T. J. Meyer, *Inorg. Chem.* **1978**, *17*, 3334–3341.
- [37] J. R. Alston, S. Kobayashi, T. J. Younts, J. C. Poler, *Polyhedron* **2010**, *29*, 2696–2702.
- [38] K. Warnmark, J. A. Thomas, O. Heyke, J.-M. Lehn, *Chem. Commun.* **1996**, 701–702.

Received: October 23, 2012

Revised: March 19, 2013

Published online: ■ ■ ■, 0000

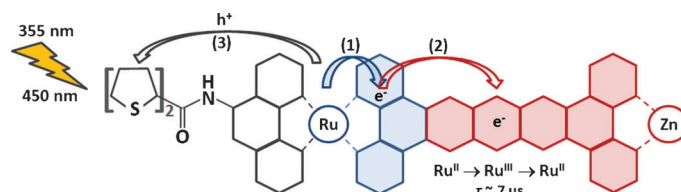
Photochemistry

M. B. Majewski, N. R. de Tacconi,

F. M. MacDonnell,*

M. O. Wolf* ■■■■-■■■■

Long-Lived, Directional Photoinduced Charge Separation in Ru^{II} Complexes Bearing Laminate Polypyridyl Ligands



Ru enlightened: Long-lived, directional photoinduced charge separation in Ru^{II} complexes with laminate polypyridyl ligands is demonstrated.

Charge separated states are exhibited by complexes bearing laminate acceptor and bithienyl donor ligands

(see scheme). Unusual excited state lifetimes reflect equilibration of ³MLCT_{prox} or ³MLCT_{dist} states with a ³LC state or a ³ILCT state that formally localizes a hole on the bithiophene and an electron on the laminate acceptor ligand.